https://doi.org/10.5194/amt-2021-221
Preprint. Discussion started: 17 August 2021

Atmospheric Measurement Techniques Discussions

An adaptive echo attenuation correction method for airborne Ka-band precipitation cloud radar based on melting layer

Dongfei Zuo[1,2], Deping Ding[3], Yichen Chen[3], Ling Yang[1,2], Delong Zhao[3], Mengyu Huang[3], Ping Tian[3], Wei Xiao[3], Wei Zhou[3], Yuanmou Du[3], and Dantong Liu[4]

[1]Chengdu University of Information Technology, Chengdu, 610225, China
[2]CMA Key Laboratory of Atmospheric Sounding, Chengdu, 610225, China
[3]Beijing Weather Modification Office, Beijing, 100089, China
[4]Department of Atmospheric Sciences, School of Earth Sciences, Zhejiang University, Hangzhou, 310058, China

Correspondence to: Deping Ding (zytddp@vip.sina.com), Yichen Chen (chenyichen@bj.cma.gov.cn)

Abstract. In this study, an airborne Ka-band Precipitation Cloud Radar (KPR) is used to carry out a cloud observation experiment. By analyzing the attenuation of the snow echo, it is found that during the snowfall, due to the low liquid water content, the KPR attenuation is small on the detection path, and after preliminary comparative analysis, the maximum attenuation correction value is 0.5dBZ. According to the echo attenuation analysis of mixed precipitation, the melting layer is found to be the key factor affecting the attenuation correction. This study hereby proposes an adaptive echo attenuation correction method based on the melting layer (AEC), and uses the ground-based S-band radar to extract the echo on the aircraft trajectory to verify the correction results. The results show that the echo attenuation correction value above the melting layer is related to the flight position. The aircraft above the melting layer is dominated by ice particles, with small attenuation correction value, the maximum correction amount of 0.13dBZ; when the aircraft is at and just below the melting layer, a water film is prone to be on the antenna, which leads to serious attenuation of the KPR detection path, with the attenuation correction value 1~2dBZ. For the precipitation echo below the melting layer, due to the abundant rain and water vapor content, the KPR attenuation is significant with maximum correction value of about 5dBZ. Compared with the S-band radar, before attenuation correction, the total mean relative error is 15%, and the correlation coefficient is 0.82; after correction, the total mean relative error is 6%, and the correlation coefficient is 0.90, indicating the significant improvement of the KPR data quality.

1 Introduction

Cloud is an important factor affecting weather and an important condition for climate formation (Fox et al., 1997). In recent years, many scholars have conducted relevant research and analysis on cloud microphysical parameters (Mace et al., 2000; Austin et al., 2009; Kim et al., 2010), which is of great significance for the study of cloud formation, precipitation prediction, and operation command of weather modification. Millimeter wave cloud radar is the main method for cloud parameter detection, at present, ground-based cloud radar is mostly used to analyze and study cloud parameters, but ground-based cloud radar can only detect cloud information at a fixed position, and cannot obtain information about the entire cloud in

https://doi.org/10.5194/amt-2021-221
Preprint. Discussion started: 17 August 2021


Atmospheric Measurement Techniques Discussions

time, the airborne detection equipment (KPR, online probe) can perform real-time cloud detection (Pazmany et al., 2008; Pazmany et al., 2018; Baker et al., 2006), which has extremely flexibility and effectiveness. The use of airborne detection equipment for joint observation provides a better method for studying cloud microphysics (Lawson et al., 2009; Zong et al., 2013). Regardless of ground-based cloud radar or airborne cloud radar, because the millimeter wave wavelength (Ka-band 8.6mm and W-band 3.2mm) is short, the electromagnetic signal on the detection path is easily attenuated, resulting in the echo intensity detected by the radar being less than the true echo, which will cause errors in the subsequent inversion of cloud microphysical parameters by the cloud radar. Therefore, it is necessary to correct the attenuation of the millimeter wave cloud radar echo.

Atlas and Banks et al. (1951) showed there were two main factors resulting in attenuation. One is detection range, whereby the echo power received by the radar will decrease with increasing range, and this applies to all radar wavelengths; the other is rain attenuation, Hitschfeld et al. (1954) and Ulbrich et al. (1983) proposed to use the empirical formula between the radar reflectivity factor z and the attenuation coefficient k to correct the attenuation of the centimeter wave weather radar (Hildebrand et al., 1978; Johnson et al., 1987), which is also the mainstream algorithm for the current radar echo attenuation correction. Meneghini et al. (1978) discussed the relationship between the attenuation analytical correction method and the iterative method. Lhermitte et al. (1990) studied the attenuation and scattering of millimeter wavelength radiation by clouds and precipitation. Shinta Seto et al. (2015) proposed an analytical method for the dual-frequency rainfall radar (DPR) on the global rainfall measurement (GPM) core observatory, and adjusted the k-z relationship coefficient based on the dual-frequency reflectance ratio and surface reference technology. Zhang et al. (2001) derived the attenuation correction method by bin-by-bin, bin-by-bin approximation and stability judgment based on the relationship between radar reflectivity factor and attenuation coefficient. Wang et al. (2011) obtained the relationship between the attenuation coefficient and reflectivity factor of the W-band and Ka-band cloud radar detecting spherical cloud and precipitation particles according to the calculation formula of the Mie scattering theory. Through numerical simulation, the four types of non-precipitation clouds were analyzed, the echo of the airborne W-band radar has been attenuated and corrected (Wang et al. 2011). Wu et al. (2013) studied the relationship between the attenuation coefficient of non-spherical ice crystals and the equivalent reflectivity factor of cloud radar. According to the difference of cloud echo intensity, Huang et al. (2013) and Yao et al. (2019) revised the echo intensity of 35GHz cloud radar based on the empirical relationship of $k = aZ^b$ for different types of clouds by using the hierarchical bin-by-bin correction method. In order to correct the attenuated millimeter wave (Ka-band) radar echo and solve the instability problem, Zhang et al. (2016) proposed an attenuation correction method (attenuation correction with change trend constraint; VTC), the X-band weather radar is used to compare and verify the correction results. This method can avoid the instability problem caused by the lack of constraints in the conventional bin-by-bin correction method.

The current correction algorithm for radar echo attenuation is mainly for ground-based radar echo attenuation correction, due to the lack of airborne cloud radar in China, there are relatively few related studies. In this paper, the attenuation correction of a snowfall process is carried out based on the bin-by-bin attenuation correction method, and the radar echo on the aircraft trajectory extracted by the ground-based S-band radar is compared and analyzed to eliminate the systematic error between

https://doi.org/10.5194/amt-2021-221
Preprint. Discussion started: 17 August 2021


Atmospheric Measurement Techniques Discussions

the KPR and the S-band radar. Then, on the basis of the method of bin-by-bin correction, an adaptive attenuation correction method based on the melting layer is proposed to attenuate the mixed precipitation echo, the results show that the echo quality after KPR attenuation correction is significantly improved.

2 Instruments introduction

The airborne Ka-band precipitation cloud radar is an airborne cloud radar (ProSensing Inc., US). KPR is a compact, dual-beam, solid-state transmitter Doppler radar (Figure 1). The specific parameters of KPR are shown in Table 1. It has two antennas, one pointing upwards and the other pointing downwards, it uses a linearly polarized flat panel array for measurements above and below the aircraft, and can continuously observe the changes in the horizontal and vertical structure of the cloud. The working center frequency is 35.64GHz, and the radar wavelength is about 8.42mm. KPR uses the standard pulse pair algorithm to measure the following quantities: Reflectivity (dBZ), Doppler velocity, and Doppler width.

Figure 1. KPR installed on wing of King Air.

Table 1. KPR specifications

Parameter	Specification
Frequency	35.64 GHz +-30 MHz
Peak Power	10W
Maximum Transmitter Duty Cycle	10 %
Maximum Pulse Repetition Frequency	20 kHz
TX Pulse Length	100 ns~10μs
Antenna Gain	32.5dBi
Beam width	4.2°
Antenna First Side lobe Level	-23 dB
LNA Noise Figure	3 dB
Data Products	Reflectivity, Doppler velocity, and Doppler spectral width

https://doi.org/10.5194/amt-2021-221
Preprint. Discussion started: 17 August 2021

Atmospheric Measurement Techniques Discussions

The airborne weather detection system AIMMS-20 (Figure 2) can be used for the observation of temperature, humidity, wind 3D spatial conditions, and airflow during flight. The instrument includes an air data probe (ADP), which measures airflow and air temperature and humidity through a differential pressure and countercurrent temperature/humidity measurement room; an inertial measurement unit (IMU) measures the altitude of the mid-top aircraft on the entire track; GPS measures the altitude of the aircraft and the fuselage slope.

Figure 2. Airborne weather detection system AIMMS-20

S-band Doppler weather radar for Beijing and Zhangjiakou, operating at 2.7GHz~3.0GHz, the volume scanning cycle is no more than 6 minutes, and the observation mode can be automatically changed according to the actual weather.

First, according to the AMIMIS-20 probes on board the aircraft, the time, latitude, longitude, and altitude of the flight are obtained to match S-band radar volume scan data, obtain the S-band radar echo of the vertical profile on the aircraft trajectory. The range gate spacing of KPR is 15m and the time resolution is 0.2s, the S-band radar echo on the flight trajectory extracted by the AMIMIS-20 probe has a lower resolution, and the S-band radar echo is interpolated to adjust the resolution of the two radars to be consistent. Then the KPR echo data is attenuated and corrected, and compared with the echo data on the aircraft trajectory extracted by the ground-based S-band radar.

3 Introduction to attenuation correction algorithm

3.1 The bin-by-bin attenuation correction algorithm

According to the principle of millimeter wave radar detection (Atlas et al., 1951; Zhang et al., 2001; Pazmany et al., 2017), the radar equation is:

$$P_r(R) = \frac{C}{R^2} Z_r(R)\tau(\mathrm{R}), \quad (1)$$

where, R stands for distance, $P_r(R)$ is the radar echo power, C is radar constant, $Z_r(R)$ is the true reflectivity factor at the distance R, $\tau(R)$ is the average dual-path transmittance of radar and distance R:

$$\tau(R) = e^{-2\int_0^R k(R)dR}, \quad (2)$$

https://doi.org/10.5194/amt-2021-221
Preprint. Discussion started: 17 August 2021


Atmospheric Measurement Techniques Discussions

where, *k(R)* is the attenuation coefficient, is NP/m. When the attenuation is not taken into account, Equation (1) can be written as:

$$Z_M(R) = \frac{R^2}{C} P_r(R) \,, \tag{3}$$

Where, $Z_M(R)$ is the measured value observed by radar, and can be obtained from Equations (1) and (3):

$$Z_M(R) = Z_r(R)\tau(R) \,, \tag{4}$$

The empirical formula between attenuation coefficient k and radar reflectivity factor Z can be expressed as:

$$k = aZ^b, \tag{5}$$

Therefore, it can be obtained:

$$Z_M(R) = Z_r(R)\mathrm{e}^{-2\int_0^R aZ_r(R)^b dR}, \tag{6}$$

In radar observation, the reflectivity obtained by the radar is corresponding to its radial range gates, and the range resolution is ΔR, the distance from the radar to the center of the i-th range gate is (i-0.5) ΔR, the corresponding radar reflectivity is $Z_M(i)$, the integral average value within the i-th range gate is:

$$Z_M(i) = \frac{1}{\Delta R}\int_{(i-1)\Delta R}^{i\Delta R} Z_M(R)dR, \tag{7}$$

The corresponding discrete form is:

$$Z_M(i) = Z_r(i)\tau_i, \tag{8}$$

Which can be obtained from Equations (6) and (7)：

$$\tau_i = \tau(i\Delta R) = \begin{cases} 1, & i = 0 \\ \exp\left(-2\sum_{j=1}^{i} aZ_r(j)^b \Delta R\right), & i \geq 1 \end{cases}, \tag{9}$$

When the range gate is greater than 1,

$$\tau_i = \tau_{i-1}\exp(-2aZ_r(i)^b\Delta R), \tag{10}$$

Combining Equations (8) and (10) can be obtained:

$$Z_r(i) = [Z_M(i)/\tau_{i-1}]\exp(aZ_r(i)^b\Delta R), \tag{11}$$

Equation (11) is the bin-by-bin attenuation correction method, this method estimates its true value based on the reflectivity value observed by the radar. KPR is different from the ground-based cloud radar. It has two antennas, which are based on the flight position of the aircraft and transmit signals upward and downward at the same time, while the ground-based cloud radar is based on the ground and sends signals upward. In the attenuation correction of KPR, the altitude of the aircraft is taken as the starting range gates, hereinafter the attenuation correction for each range gate away from the aircraft altitude is performed using the bin-by-bin attenuation correction method successively.

https://doi.org/10.5194/amt-2021-221
Preprint. Discussion started: 17 August 2021


Atmospheric Measurement Techniques Discussions

3.2 The hierarchical bin-by-bin attenuation correction algorithm

The hierarchical bin-by-bin attenuation correction method divides the echo intensity into different levels and selects different attenuation coefficients according to the different radar echo intensities, so as to better take into account the different strengths of the echo, the correction effect is better. According to the research of Huang et al. (2013), the echo intensity can be divided into 5 intervals according to dBZ:

1. Weak cloud area: Z<-20 dBZ
2. Thick clouds area: -20 dBZ≤Z<0 dBZ，(a, b)=$(1.982 \times 10^{-6}, 1.13)$
3. Cloud contains liquid water: 0 dBZ≤Z<15 dBZ，(a, b)=$(1.286 \times 10^{-6}, 1.105)$
4. Weak precipitation area: 15 dBZ≤Z<25 dBZ，(a, b)=$(1.753 \times 10^{-6}, 1.075)$
5. Significant precipitation area: Z≥25dBZ，(a, b)=$(1.304 \times 10^{-6}, 1.040)$

According to different intensity levels, different attenuation coefficients are selected to attenuate the radar echo, for weak echoes with echo intensity less than -20dBZ, the cloud radar is almost unaffected, so no correction processing is performed.

3.3 Adaptive echo attenuation correction algorithm based on melting layer

In the case of snowfall, the water vapor content is low and the attenuation is relatively weak, the echo intensity is generally no more than 20dBZ, but it is attenuated more than non-precipitation weak clouds, through the analysis of experimental data, this paper chooses a fixed attenuation coefficient $(1.304 \times 10^{-7}, 1.04)$ is selected for the snowfall echo to correct the attenuation by using the bin-by-bin correction method.

In mixed precipitation clouds, there are particles in multiple phases, below the melting layer, electromagnetic waves will be severely attenuated when encountering abundant water vapor, for echoes above the melting layer, the particle forms are mostly ice phases (ice crystals, snowflakes), the liquid water content is low and the attenuation is relatively weak. So, for mixed precipitation echo, this paper proposes an adaptive echo attenuation correction method based on melting layer.

The adaptive echo attenuation correction method based on the melting layer (Figure 3), firstly obtain the height of the melting layer according to the aircraft altitude and temperature recorded by the airborne AIMMS-20 probe, and then determine the position relationship between the aircraft and the melting layer, according to the melting layer to transform different correction coefficients. For the echo above the melting layer, choose the same attenuation coefficient $(1.304 \times 10^{-7}, 1.04)$ as the snowfall and use the bin-by-bin attenuation correction method. For the echo below the melting layer, according to the different intensity of the echo, different attenuation coefficients are selected to correct from the bin-by-bin, that is, the hierarchical bin-by-bin correction method.

https://doi.org/10.5194/amt-2021-221
Preprint. Discussion started: 17 August 2021

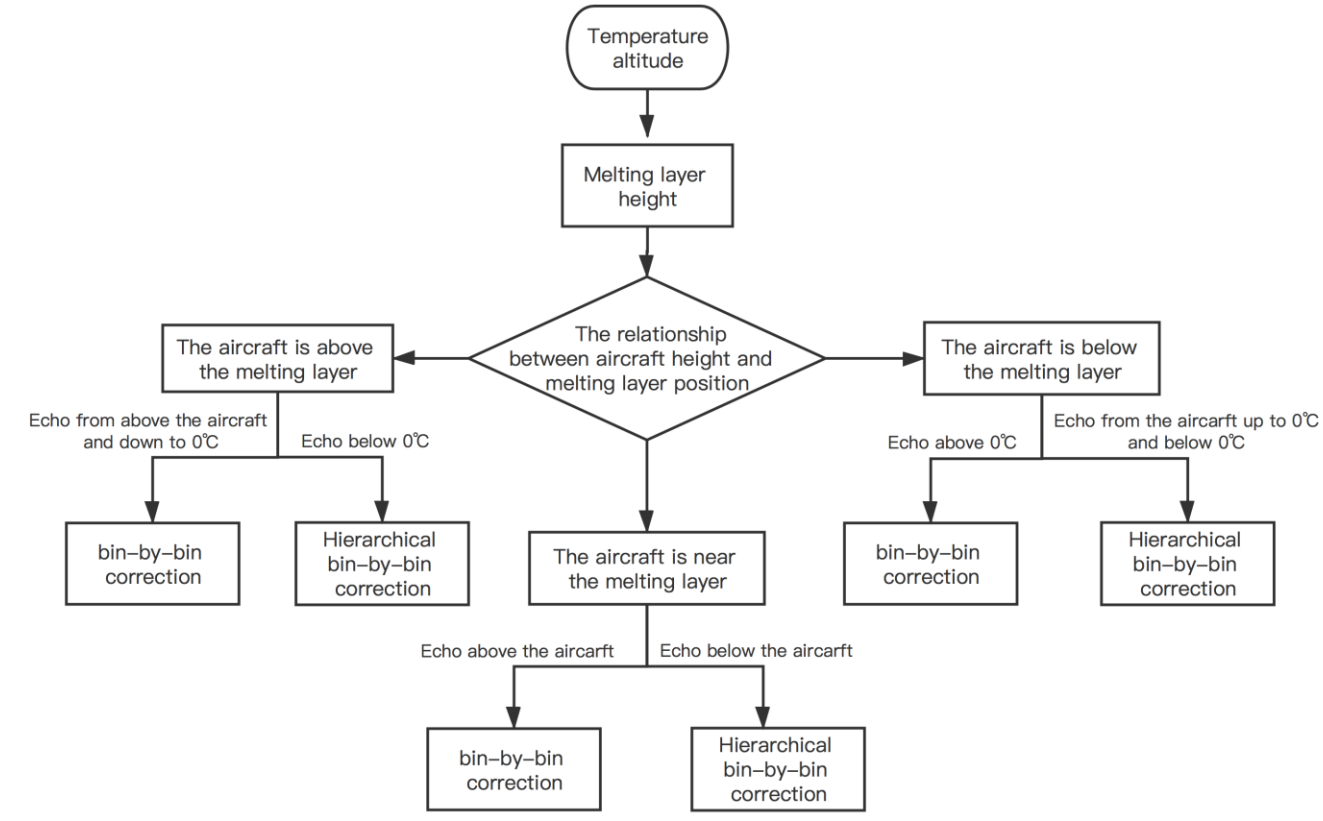

Figure 3. An adaptive echo attenuation correction algorithm based on the melting layer

4 Analysis of snowfall echo attenuation correction results

Figure 4 shows a snowfall observed from on 29 November, 2019, 10:25-10:52 (UTC) in Zhangjiakou, the radar echoes are evenly distributed, the echo top height is low, and the cloud top height detected by KPR is about 5km, the horizontal detection distance is 120km. During the period of 10:25-10:37, the maximum radar echo is 15dBZ, during the period of 10:37-10:52, the radar echo is weak, at -1~8dBZ.

Considering the difference in cloud top height detected by KPR and S-band radar, this paper selects the radar echo intensity at four altitude layers of 2.5km, 2.8km, 3.1km, and 3.4km for analysis and explanation. Figure 5 shows the detection results of KPR and S-band radar echo data at four different altitude layers. Table 2 is the average of KPR and S-band radar echo data at four different altitude layers, and the following statistics are obtained:

https://doi.org/10.5194/amt-2021-221
Preprint. Discussion started: 17 August 2021

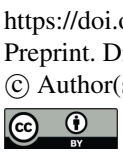

Atmospheric Measurement Techniques Discussions

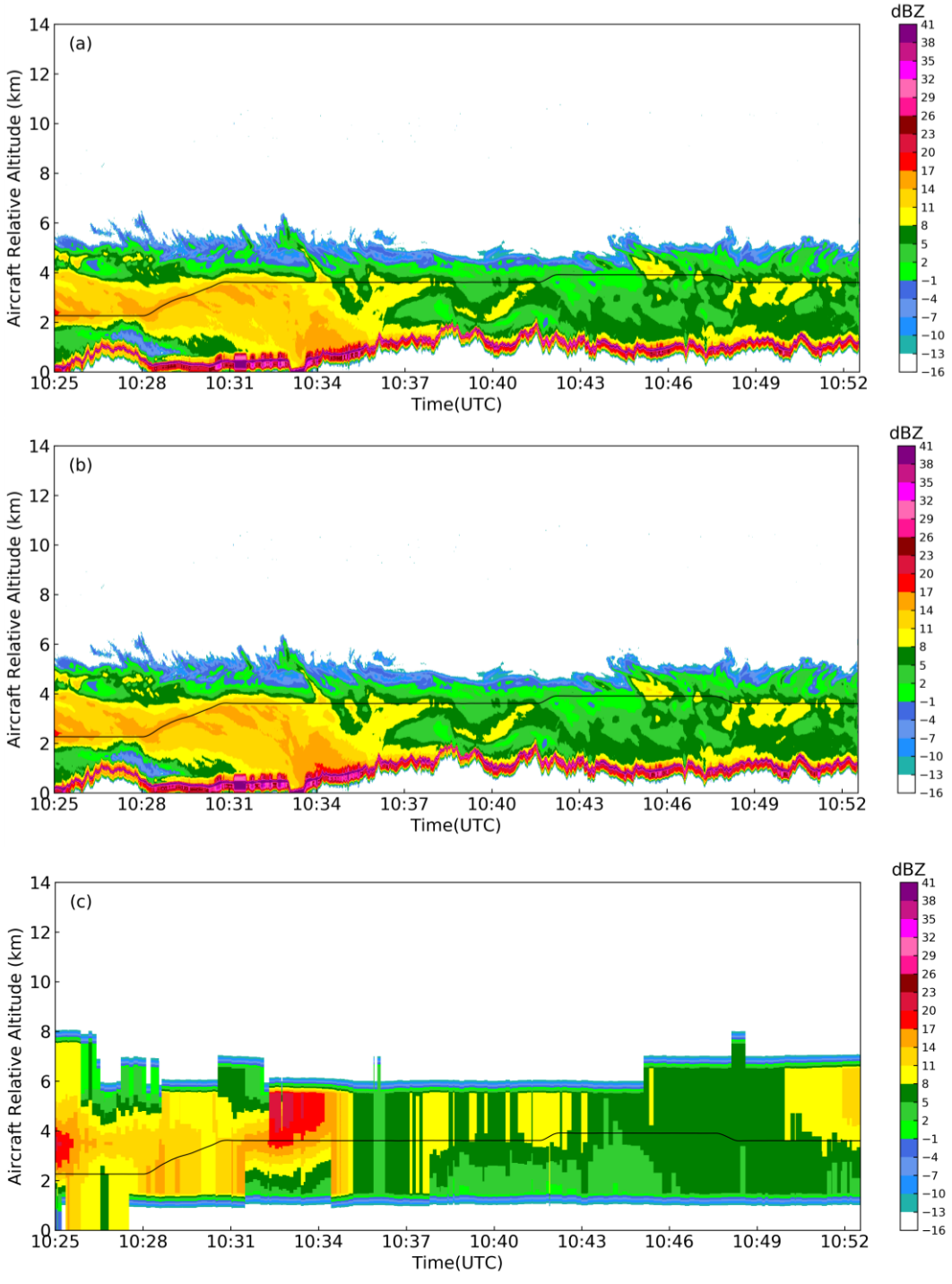

Figure 4. KPR radar echo before and after attenuation correction and S-band radar echo under snowfall conditions (a. KPR radar echo before attenuation correction, b. KPR radar echo after attenuation correction, c. S-band radar echo)

https://doi.org/10.5194/amt-2021-221
Preprint. Discussion started: 17 August 2021


Atmospheric Measurement Techniques Discussions

Table 2. The average value of S-band radar echo and KPR echo under different altitude layers under snowfall conditions (unit: dBZ)

Height	S-band	KPR Uncorrected	KPR corrected
2.5km	8.51	8.20	8.32
2.8km	8.62	8.69	8.80
3.1km	9.04	8.62	8.72
3.4km	9.43	8.81	8.88

It can be seen from Table 2 that in the case of snowfall, the value of attenuation correction is small, and the correction value is the largest at the 2.5km altitude layer, which is 0.12dBZ, the correction value at the altitude layer of 2.8km, 3.1km, and 3.4km decreases in turn, which are 0.11dBz, 0.10dBz and 0.07dBz respectively. The S-band radar echo intensity is 0.19dBZ, -0.18dBZ, 0.32dBZ, and 0.75dBZ larger than the corrected average value of KPR attenuation, respectively, and the corrected error is about 1dBZ. KPR echo before and after the correction is basically the same as the S-band radar (Figure 5), at the 3.4km altitude layer, the S-band radar echo intensity is quite different from the KPR (Figure 5d), during the period of 10:37-10:49, the S-band radar echo is about 3dBZ larger than the KPR as a whole, which may be caused by the inaccurate interpolation of the S-band radar, but the overall trend of the two radars is the same.

The previous description is mainly for radar echoes at different heights, in order to better understand the attenuation changes of KPR on the detection path, the average echo profile of two periods 10:31-10:34 and 10:46-10:49 are selected (Figure 6) for analysis and explanation. From Figure 5, the radar echo intensity is relatively high in the period of 10:31-10:34, around 15dBZ, and the aircraft altitude is 3600m. It can be seen from Figure 6a that the value of KPR attenuation correction is increasing under the aircraft, the maximum value is 0.5dBZ, above the aircraft, due to the small echo intensity, the detection

https://doi.org/10.5194/amt-2021-221
Preprint. Discussion started: 17 August 2021

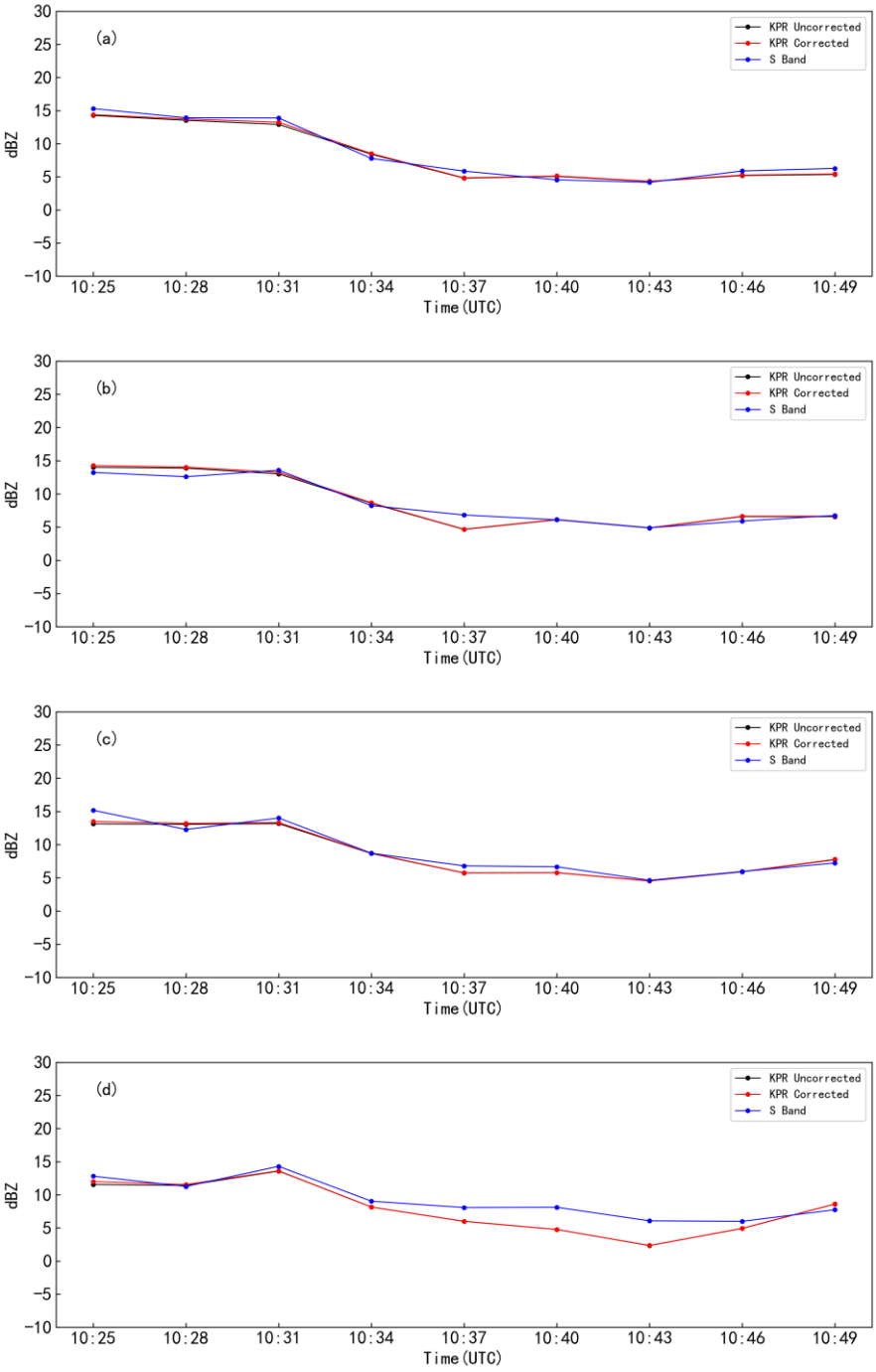

Figure 5. KPR echoes before and after attenuation correction and S-band radar at different altitudes (a.2.5km altitude echo intensity, b.2.8km altitude echo intensity, c.3.1km altitude echo intensity, d.3.4 km height layer echo intensity)

path is closer to the aircraft, and the maximum attenuation correction value is only 0.01dBZ, which is almost unchanged from the echo profile. Above 3.5km, the KPR echo profile is quite different from the S-band, which may be caused by the

https://doi.org/10.5194/amt-2021-221
Preprint. Discussion started: 17 August 2021

Atmospheric Measurement Techniques Discussions

low spatial resolution of the S-band radar and inaccurate interpolation results. During the period of 10:46-10:49, the radar echo is weak, at about 5dBZ, and the aircraft altitude is 3900m, from the average echo profile at this moment, the attenuation correction value at the entire altitude is small, and the maximum attenuation value is only 0.09dBZ at 2km, the KPR profile is "S-shaped", and the echo intensity is between 5-6dBZ, the echo intensity of the S-band radar is about 5.9dBZ, the overall difference between the two radars is small, it has a good correspondence with echoes at different heights as shown in Figure 5.

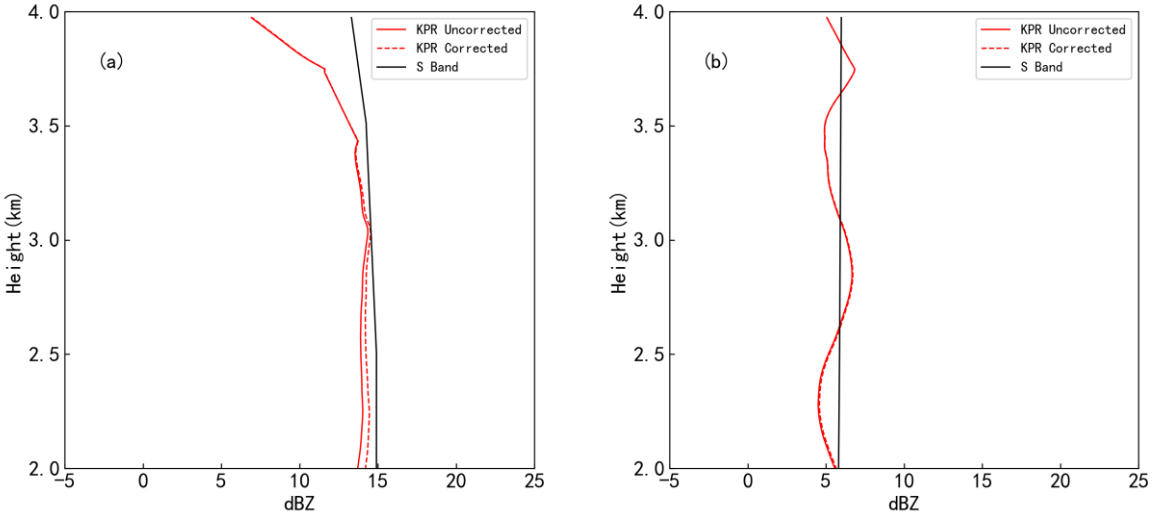

Figure 6. 2-4km the average echo intensity profile (a.10:31-10:34 echo intensity profile, b.10:46-10:49 echo intensity profile)

4 Analysis of mixed precipitation cloud echo attenuation correction results

4.1 Comparative analysis of echo intensities at different altitude layers

Figure 7 is the radar echo observed during the period of horizontal aircraft flight on 22 June, 2020, 04:53-05:17 (UTC), it can be seen from Figure 7a that the height of the cloud top detected by KPR is about 6km, the horizontal detection distance is about 110km, the height of the melting layer is about 4100m, and the aircraft is located below the melting layer. The KPR echo before and after the attenuation correction has a good corresponding relationship with the S-band radar echo.

https://doi.org/10.5194/amt-2021-221
Preprint. Discussion started: 17 August 2021

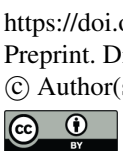

Atmospheric Measurement Techniques Discussions

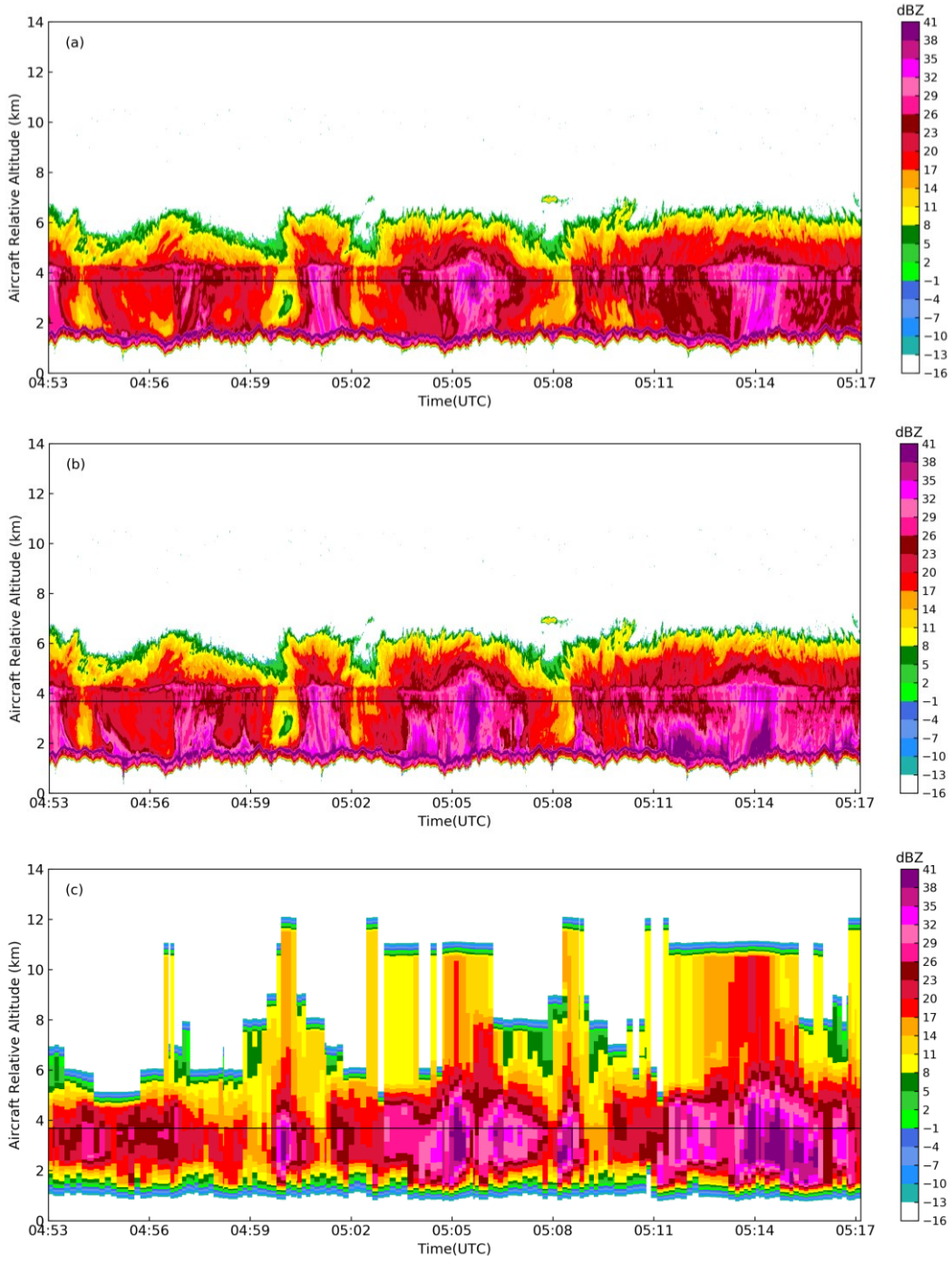

Figure 7. Flight time 1 KPR radar echo before and after attenuation correction and S-band radar echo (a. KPR radar echo before attenuation correction, b. KPR radar echo after attenuation correction, c. S-band radar echo)

https://doi.org/10.5194/amt-2021-221
Preprint. Discussion started: 17 August 2021

Atmospheric Measurement Techniques Discussions

According to the results obtained in Table 3, the S-band radar echo intensity at the four altitude layers is respectively 4.7dBz, 3.28dBz, 1.07dBz and 1.41dBz larger than the average value before KPR attenuation correction, and 0.32dBz, 1.15dBz, 1.29dBz and 0.55dBz larger than after KPR attenuation correction, respectively. It can be seen from the statistical value that the quality of echo intensity after the correction of KPR attenuation is obviously improved, and the average deviation from S-band radar is about 1dBz.

It can be seen from Figure 8 that the echo intensity after the KPR attenuation correction is basically the same as that of the S-band radar. During this flight period, the flight altitude is about 3800m, and the 3.5km and 4.5km altitude layer are relatively close to the aircraft, the attenuation correction does not change much, the average difference of the echo intensity at this altitude before and after the correction is 0.41dBZ and 0.88dBZ, respectively. The 2.5km and 3.0km altitude layer are far away from the aircraft, under rain conditions, the water vapor content is abundant, and the attenuation on the radar detection path is relatively large, the average difference of echo intensity before and after correction is 4.38dBZ and 2.13dBZ, respectively.

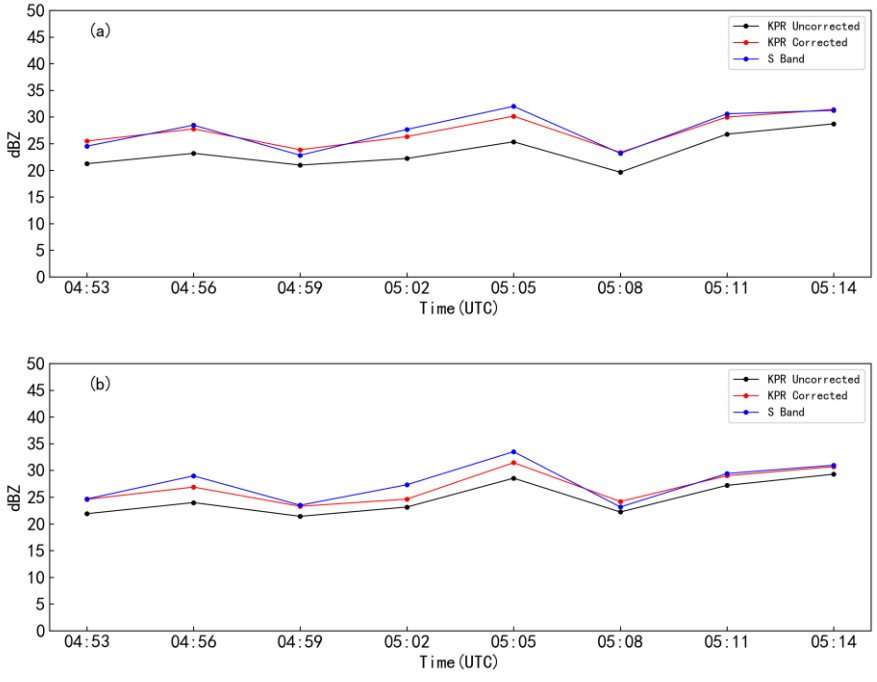

https://doi.org/10.5194/amt-2021-221
Preprint. Discussion started: 17 August 2021

Atmospheric Measurement Techniques Discussions

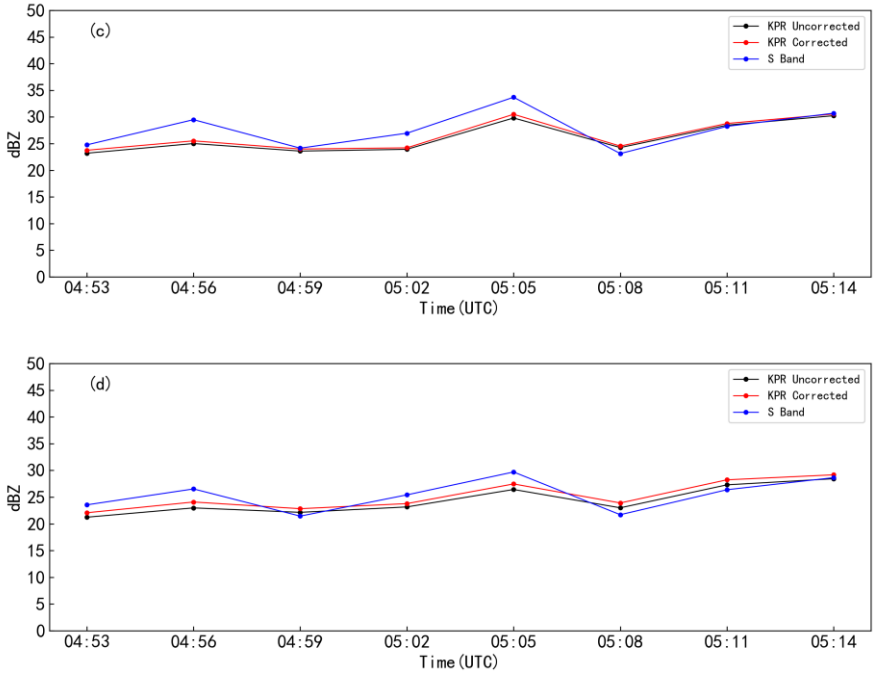

Figure 8. KPR before and after attenuation correction and S-band radar echo at different altitude layers (a.2.5km altitude echo intensity, b.3.0km altitude echo intensity, c.3.5km altitude echo intensity, d.4.5 km height layer echo intensity)

Figure 9 is the radar echo observed during the plane's level flight on 22 June, 2020, 05:40-05:56 (UTC), the height of the cloud top detected by KPR is 8km, the height of the melting layer is about 4000m, and the aircraft is above the melting layer, The horizontal detection distance is about 80km.

During this period, the height of the cloud top detected by KPR is about 8km, and the height of the aircraft is 5km, however, due to the low spatial resolution of the S-band radar, the height of the cloud top obtained after interpolation is 12km, therefore, this paper focuses on analyzing the radar echo below 6km, the radar echo intensity of four different altitude layers of 2.5km, 3km, 3.5km, and 5km are selected for analysis and explanation. Figure 10 shows the detection results of KPR and S-band radar echo data at four different altitude layers. Table 4 is the average value of KPR and S-band radar echoes at four different altitudes, and the following statistics are obtained:

https://doi.org/10.5194/amt-2021-221
Preprint. Discussion started: 17 August 2021

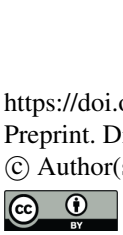

Atmospheric Measurement Techniques Discussions

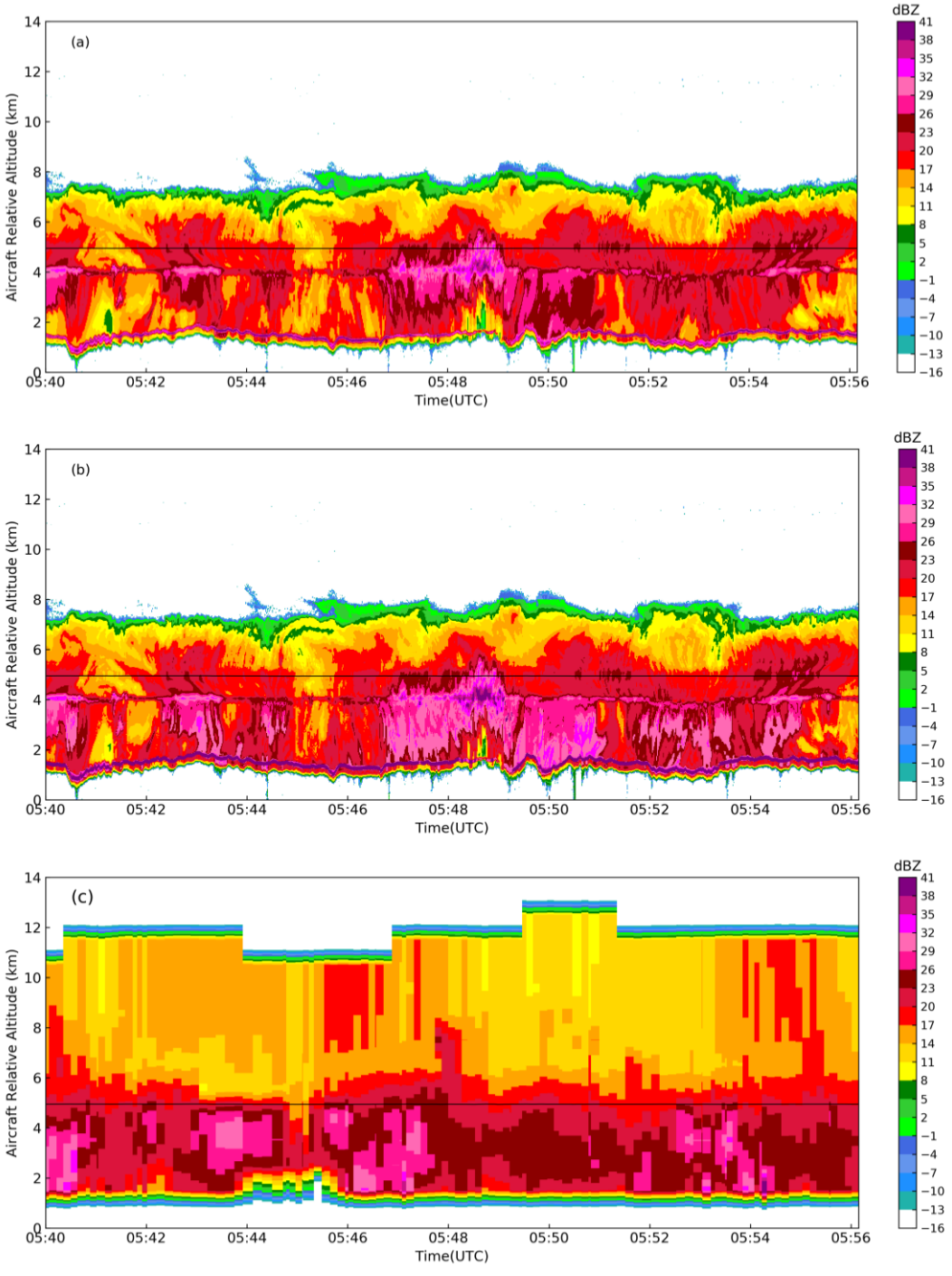

Figure 9. Flight time 2 KPR radar echo before and after attenuation correction and S-band radar echo (a. KPR radar echo before attenuation correction, b. KPR radar echo after attenuation correction, c. S-band radar echo)

https://doi.org/10.5194/amt-2021-221
Preprint. Discussion started: 17 August 2021

Atmospheric Measurement Techniques Discussions

Table 4. Flight time 2 the average value of S-band radar echo and KPR echo at different altitude layers (unit: dBZ)

Height	S-band	KPR Uncorrected	KPR corrected
2.5km	24.74	19.23	23.54
3.0km	24.99	20.63	24.30
3.5km	25.24	21.74	23.65
5.0km	20.62	20.77	20.77

According to the results obtained in Table 4, the S-band radar echo intensity at the four altitude layers is 5.51dBz, 4.36dBz, 3.5dBz and -0.15dBz larger than the average value before KPR attenuation correction, respectively, and 1.2dBz, 0.66dBz, 1.59dBz and -0.15dBz larger than the average value after KPR attenuation correction, respectively. It can be seen from the statistical value that the quality of echo intensity after the correction of KPR attenuation is obviously improved, and the difference between KPR attenuation and S-band radar is about 1dBz.

The flight altitude during this flight period is about 5000m, it can be seen from Figure 10d that the attenuation correction is almost unchanged when the 5.0km altitude is on the aircraft's trajectory, while the 2.5km, 3.0km, and 3.5km altitudes are far away from the aircraft, and below the melting layer, the water vapor content is rich, the attenuation is larger, and the average difference of echo intensity before and after correction is 4.31dBZ, 3.67dBZ and 1.91dBZ, respectively.

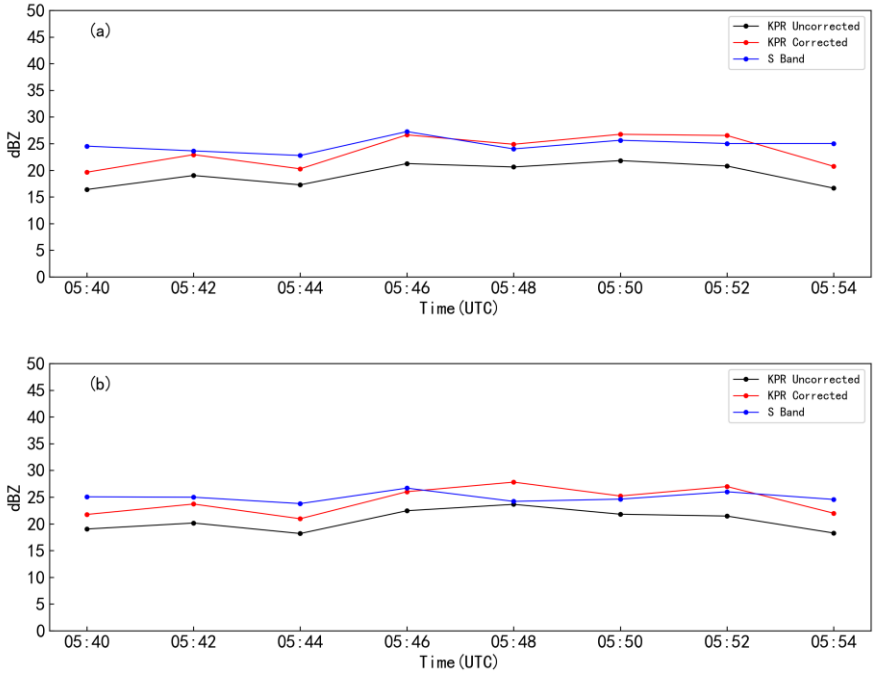

https://doi.org/10.5194/amt-2021-221
Preprint. Discussion started: 17 August 2021

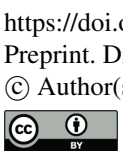

Atmospheric Measurement Techniques Discussions

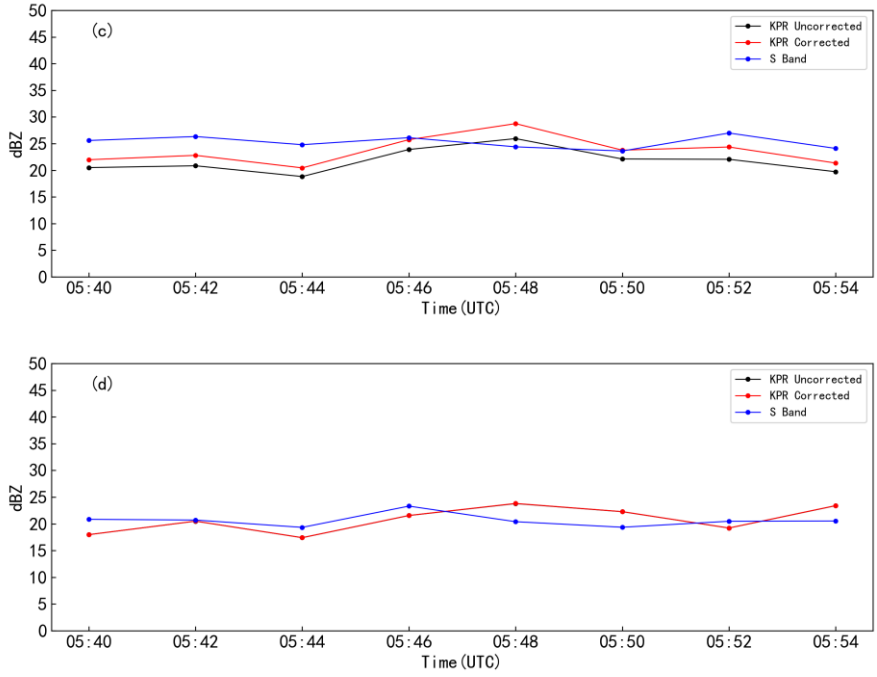

Figure 10. KPR before and after attenuation correction and S-band radar echo at different altitude layers (a.2.5km altitude echo intensity, b.3.0km altitude echo intensity, c.3.5km altitude echo intensity, d.4.5 km height layer echo intensity)

Figure 11 is the radar echo observed during the plane's level flight on 22 June, 2020, 06:10-06:28 (UTC), the difference between the KPR radar echo and the S-band radar echo during this period compared with the previous two periods slightly larger, affected by the attitude and circling angle of the aircraft, resulting in a big difference in matching with the S-band radar data, but the overall consistency remains the same. The height of the cloud top detected by KPR during this period was about 8km, and the height of the aircraft was near the melting layer.

For this period, this paper selects the radar echo intensity of 2.5km, 3km, 3.5km, and 5km for analysis and explanation. Figure 12 shows the detection results of KPR and S-band radar echo data at four different altitude layers. Table 5 is the average value of KPR and S-band radar echoes at four different altitudes, and the following statistics are obtained:

Table 5. Flight time 3 the average value of S-band radar echo and KPR echo at different altitude layers (unit: dBZ)

Height	S-band	KPR Uncorrected	KPR corrected
2.5km	25.61	20.37	22.44
3.0km	25.46	20.57	22.36
3.5km	25.32	20.61	21.69
5.0km	18.70	15.31	16.92

https://doi.org/10.5194/amt-2021-221
Preprint. Discussion started: 17 August 2021

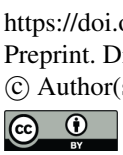

Atmospheric Measurement Techniques Discussions

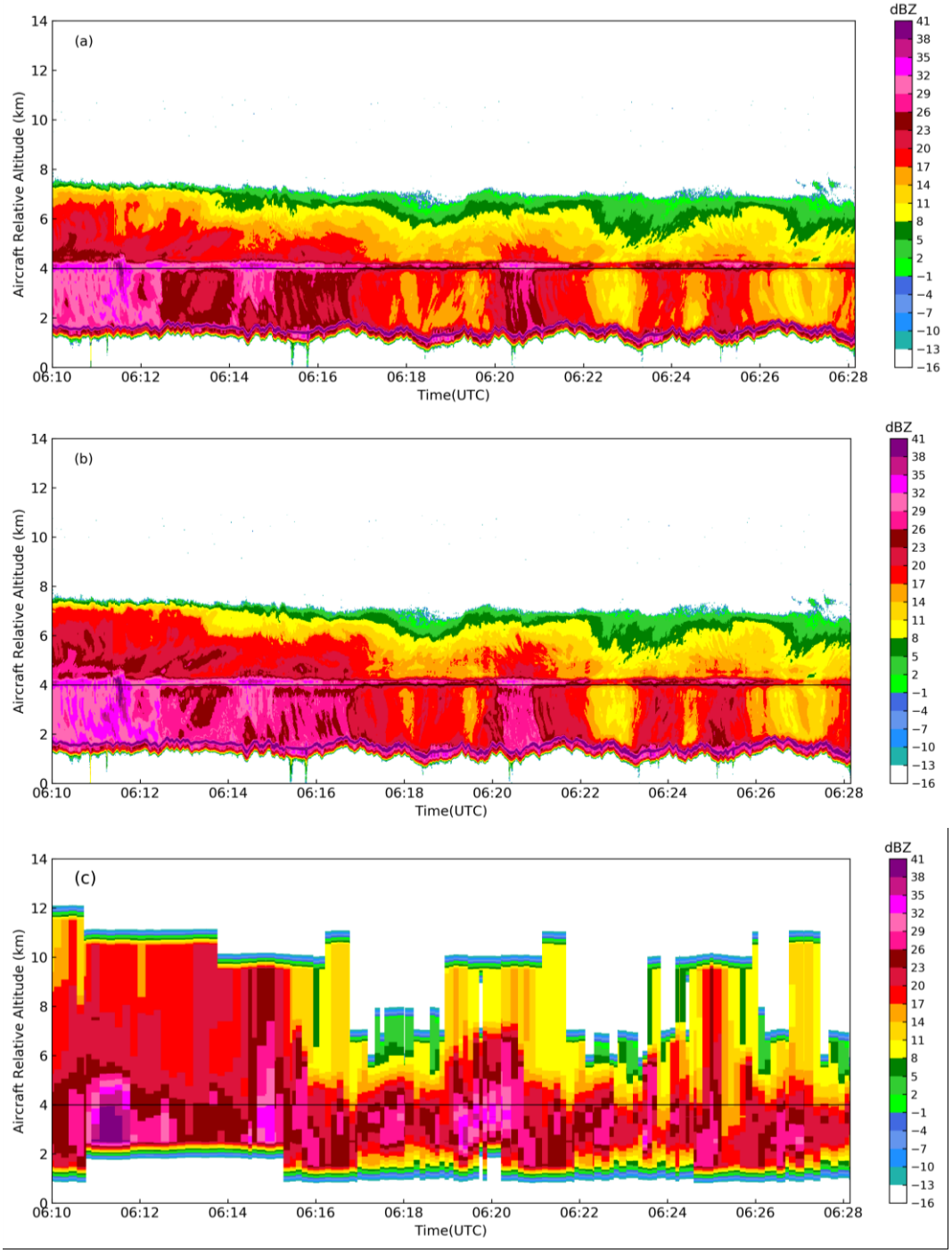

Figure 11. Flight time 3 KPR radar echo before and after attenuation correction and S-band radar echo (a. KPR radar echo before attenuation correction, b. KPR radar echo after attenuation correction, c. S-band radar echo)

https://doi.org/10.5194/amt-2021-221
Preprint. Discussion started: 17 August 2021

Atmospheric Measurement Techniques Discussions

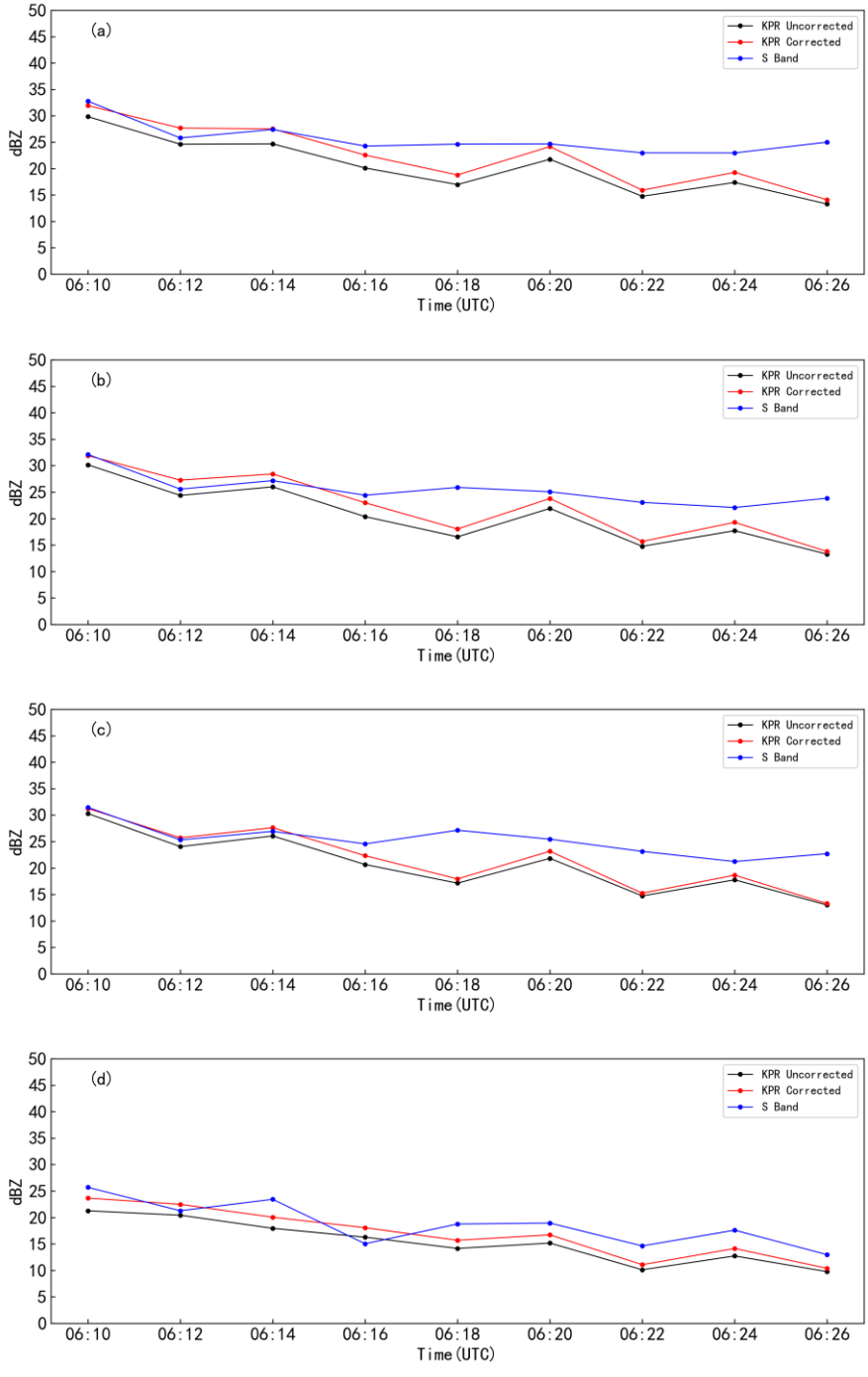

Figure 12. KPR before and after attenuation correction and S-band radar echo at different altitude layers (a.2.5km altitude echo intensity, b.3.0km altitude echo intensity, c.3.5km altitude echo intensity, d. 5.0 km height layer echo intensity)

https://doi.org/10.5194/amt-2021-221
Preprint. Discussion started: 17 August 2021

Atmospheric Measurement Techniques Discussions

According to the results obtained in Table 5, the S-band radar echo intensity at the four altitude layers are 5.24dBZ, 4.89dBZ, 4.71dBZ, 3.39dBZ larger than the average before the correction of KPR attenuation, respectively, and 3.17dBz, 3.10dBz, 3.63dBz and 1.78dBz larger than the average after the correction of KPR attenuation respectively. It can be seen from the statistical value that in this period of KPR, the difference between KPR and S-band radar echo after attenuation correction is slightly larger, about 3dBZ.

The flight altitude during this flight period is about 4000m, which is consistent with the change trend of the previous two periods, the farther away from the aircraft, the lager the difference after attenuation correction. The average difference of the echo intensity before and after the correction at the 2.5km, 3.0km and 3.5km altitude layers below the aircraft is 2.07dBZ, 1.79dBZ and 1.08dBZ, respectively, while the average difference of the echo intensity before and after the correction at the 5.0km altitude above the aircraft is 1.61dBZ.

4.2 Comparative analysis of vertical profile echo intensity

The previous comparison and analysis of the radar echo data at 4 different altitude layers in different flight periods are carried out, in order to better understand the attenuation changes of KPR on the detection path, the average echo profile at 04:56-04:58 and 05:13-05:15 in flight period 1 was selected in Figure 13 for analysis and explanation, considering that the cloud top height detected by KPR in this period is 6km, echo data at a height of 2-5km are selected for analysis.

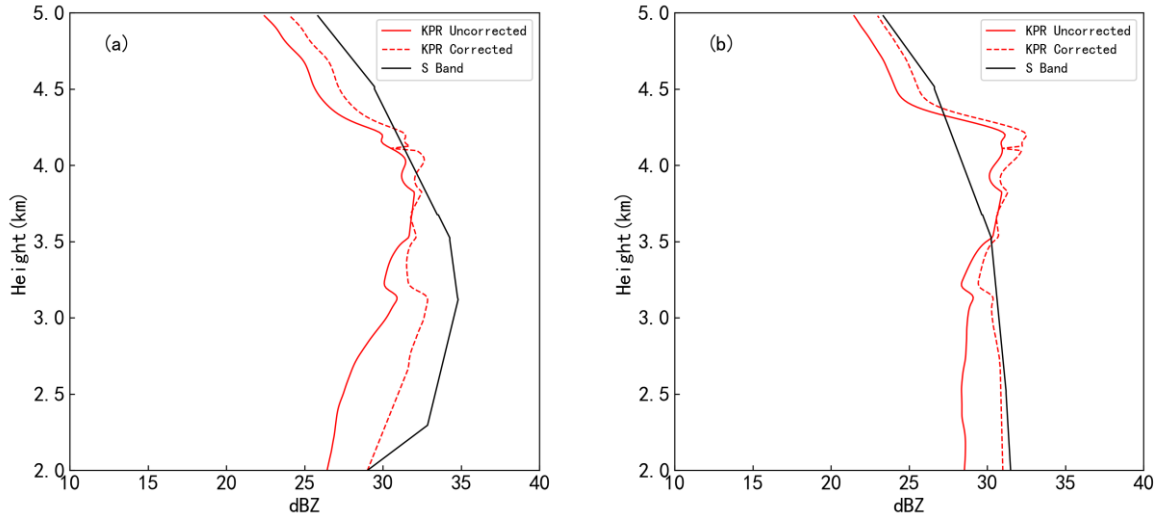

Figure 13. The average echo profile of 2-5km during flight period 1 (a.04:56-04:58 the average echo profile, b.05:13-05:15 the average echo profile)

From the average vertical echo profile at these two moments, it can be seen that the echo intensity of the KPR is consistent with the overall trend of the S-band radar, at about 3.8km (aircraft flight position), the KPR attenuation correction has little

https://doi.org/10.5194/amt-2021-221
Preprint. Discussion started: 17 August 2021


Atmospheric Measurement Techniques Discussions

change before and after the correction, in turn up or down KPR attenuation correction difference before and after the increase, the farther away from the radar, the greater the attenuation of KPR on the detection path. The height of the melting layer during this period is about 4200m, the aircraft is located below the melting layer, below the melting layer, the water vapor content is rich and the attenuation is large due to the interference of rain particles, in the distance from the aircraft, the attenuation correction value is up to 4dBZ, and the echo quality after attenuation correction is significantly improved, which is consistent with S-band radar. In Figure 13b, the echo intensity near 4.2km is larger than that of the S-band radar, this is due to the increased scattering power of electromagnetic waves when ice particles pass through the melting layer; On the other hand, because the particles collide with each other more opportunities to form larger particles, the scattering ability is further increased, so the echo on the melting layer detected by KPR is larger, while the S-band radar cannot detect the melting layer, therefore, the echo intensity of KPR near the melting layer is larger than that of the S-band radar. Because the aircraft is located below the melting layer during this period, a water film is formed on the KPR antenna, and the attenuation correction value is larger above the melting layer, and the corrected difference is about 2dBZ at a far distance above the aircraft.

Figure 14 selects the average echo profile at 05:41-05:43 and 05:46-05:48 in flight period 2 respectively. On the whole, the echo intensity of KPR is consistent with the overall trend of S-band radar, at about 4km, the intensity of KPR echo suddenly increases because KPR can detect strong echo on the melting layer, while S-band radar cannot detect the melting layer. The altitude of the aircraft during this flight period is about 5km, and the aircraft is above the melting layer, the attenuation is relatively small at 1km above and below the melting layer, at 6km, the attenuation correction value is about 0.13dBZ, which is consistent with the correction result of the snowfall process. Below the melting layer, the difference before and after the KPR attenuation correction increases, and the correction value is about 5dBZ at 2.0km. The overall echo intensity after KPR correction is consistent with that of the S-band radar.

Figure 15 selects the average echo profile at 06:11-06:13 and 06:19-06:21 in flight period 3. It can be seen from the figure that the attenuation corrected echo is consistent with the S-band radar, at about 4km, the KPR echo intensity suddenly increases because KPR can detect strong echo on the melting layer, while the S-band radar cannot detect the melting layer. In Figure 15a, the S-band radar echo value is too small at 2~2.5km, which may be due to the high altitude in this area, which caused errors when scanning by the S-band radar. During this period, the aircraft was just near the melting layer, and a water film was formed on the KPR antenna, which caused a large attenuation on the melting layer, at an altitude of 6km (2km above the aircraft), the attenuation correction value is about 1.9dBZ. Below the melting layer, the difference before and after the KPR attenuation correction increases, and the correction value is 3.6dBZ at 2.0km. After correction, the overall echo intensity is consistent with that of the S-band radar.

https://doi.org/10.5194/amt-2021-221
Preprint. Discussion started: 17 August 2021

Atmospheric Measurement Techniques Discussions

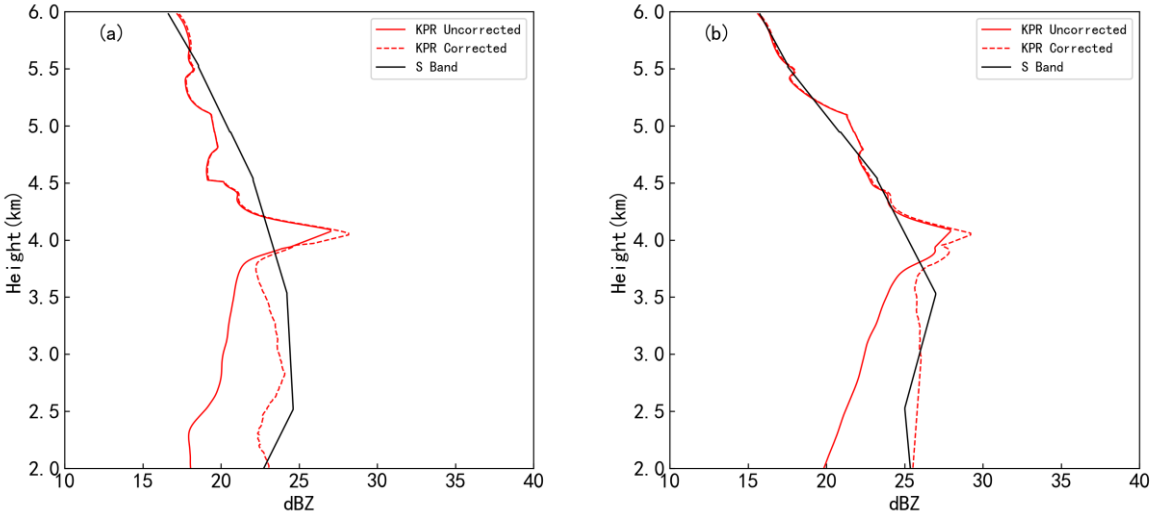

Figure 14. The average echo profile of 2-6km during flight period 2 (a.05:41-05:43 echo intensity profile, b.05:46-05:48 echo intensity profile)

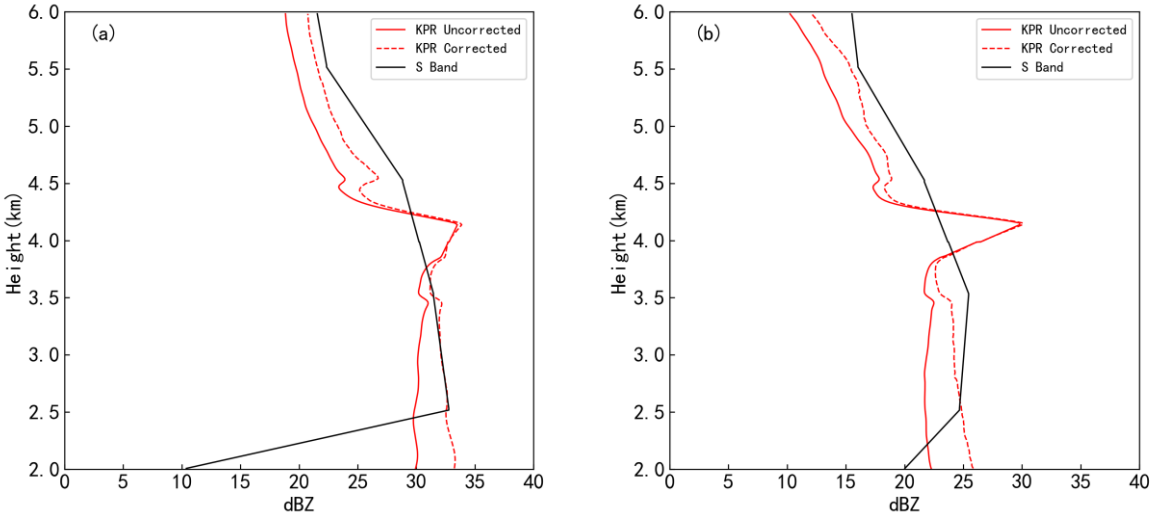

Figure 15. The average echo profile of 2-6km during flight period 3 (a.06:11-06:13 echo intensity profile, b.06:19-06:21echo intensity profile)

https://doi.org/10.5194/amt-2021-221
Preprint. Discussion started: 17 August 2021


Atmospheric Measurement Techniques Discussions

5 Conclusion and discussion

In this study, the KPR is mainly used for cloud observation, taking into account the influence of the atmosphere and water vapor on the attenuation of KPR electromagnetic wave, on the KPR detection path. As the distance increases, the electromagnetic wave transmittance becomes lower and lower, which leads to the attenuation of radar echoes seriously. In order to obtain the true echo, this paper proposes an adaptive echo attenuation correction algorithm based on the melting layer, and the following conclusions are obtained:

(1). For the snow echo, considering that the overall echo during the snowfall process is relatively weak, the water vapor content is low, the small amount of particles in the cloud attenuate electromagnetic wave, the correction amount is thus small. Even at the farthest distance from KPR, the correction amount is only 0.5dBZ.

(2). Through the attenuation correction for the snowfall cases, and the comparative analysis with the S-band radar echo, the systematic error between both radars was eliminated, and the attenuation coefficient of the snowfall attenuation correction was applied to the precipitation echo above the melting layer. The quality of the subsequent echoes has been significantly improved, which is consistent with the overall S-band radar.

(3). For mixed precipitation echo, the melting layer is the key factor affecting the attenuation correction, and the attenuation correction amount above the melting layer is related to the flight position. When the aircraft is above the melting layer, and the cloud is dominated by ice particles, the attenuation correction value is relatively small, and the maximum correction value is 0.13dBZ, while the aircraft is below the melting layer, water film is prone to appear on the antenna, which leads to serious attenuation of KPR on the detection path, and the corrected difference is about 2dBZ in the distance above the aircraft. As for the precipitation echo below the melting layer, due to the rich content of rain water and water vapor, the KPR attenuation is severe on the detection path, and the maximum correction value is up to 5dBZ.

(4). For echo of mixed precipitation clouds, this paper proposes an adaptive echo attenuation correction method based on the melting layer, through comparison and analysis with S-band radar data, this method can effectively improve the KPR echo quality. There may be convective cloud precipitation area, which results in insufficient correction value, it is also an issue that needs to be considered in the follow-up work.

KPR can perform cloud penetration detection based on information such as the position and thickness of the cloud, compared with ground-based cloud radars, the detection path is closer, the attenuation of KPR on the detection path is smaller than that of ground-based cloud radars, and it has more detection advantages. When correcting the attenuation of KPR, the attenuation correction coefficient used in this paper is based on the empirical formula summarized by Huang and others for the radar data in Yangjiang, it may not be completely applicable to the North China area. In the future, it needs to be obtained based on a large number of aircraft observation data, summarize the attenuation coefficients of different cloud systems in North China.

In addition, S-band radar data of Beijing and Zhangjiakou were used in this paper, according to the time, longitude, latitude and altitude information recorded by AIMMS-20 probe, radar echo on the trajectory of the aircraft was extracted and

compared with the corrected results of KPR attenuation, there may be some errors when matching data. Moreover, the S-band radar echo data extracted from the aircraft trajectory has a low temporal and spatial resolution, which is different from the KPR echo data.

Data availability. Data can be accessed by contacting the first author (1549620414@qq.com).

Author contribution. Deping DING has the idea, Yichen CHEN and Delong ZHAO designed the study, Dongfei ZUO worte the manuscript and the program code, Ling YANG, Mengyu Huang and Dangtong LIU gave guiding opinions on the study on the algorithm, Ping TIAN and Wei ZHOU was in charge of the flight observation, Wei XIAO and Yuanmou DU was responsible for the preprocessing of airborne detection data.

Competing interests. The authors declare that they have no conflict of interest.

Financial support. This study is supported by the National Natural Science Foundation of China.

References

Atlas, D., Banks, H. C.: The interpretation of microwave reflections from rainfall, J. Meteorol., 8, 271–282, 1951.

Austin, R. T., Heymsfield, A. J., Stephens, G, L.: Retrieval of ice cloud microphysical parameters using the CloudSat millimeterwave radar and temperature, J. Geophys. Res. –Atmos., https://doi.org/10.1029/2008JD010049, 2009.

Baker, B. A., and R. P. Lawson.: In situ observations of the microphysical properties of wave, cirrus, and anvil clouds, PartI: Wave clouds, J. Atmos. Sci., 63, 3160–3185, https://doi.org/10.1175/ JAS3802.1, 2006.

Fox NI, Illingworth, A. J.: The retrieval of stratocumulus cloud properties by ground-based cloud radar, Journal of Applied Meteorology, https://doi.org/10.1175/1520-0450, 1997.

Hildebrand, Peter H.: Iterative Correction for Attenuation of 5 cm Radar in Rain, Journal of Applied Meteorology, 17(4):508-514, https://doi.org/10.1175/1520-0450(1978)017<0508:icfaoc>2.0.co;2, 1978.

Hitschfeld, W., Bordan, J.: Errors Inherent in the Radar Measurement of Rainfall at Attenuating Wavelengths, J. Meteor, 11(1), 58-67, 1954.

Huang, X.Y., Fan, Y.W., Li, F.et al.: The attenuation correction for a 35 GHz ground-based cloud radar. Journal of Infrared & Millimeter Waves, 32(4):325-330, https://doi.org/10.3724/SP.J.1010.2013.00325, 2013.

Johnson, B. C., E. A. Brandes.: Attenuation of a 5-cm Wavelength Radar Signal in the Lahoma-Orienta Storms, Journal of Atmospheric and Oceanic Technology, 4.3:512, https://doi.org/10.1175/1520-0426(1987)0042.0.CO;2, 1987.

Kim, D.-S., Maki, M., Lee, D.-I.: Retrieval of three-dimensional raindrop size distribution using X-band polarimetric radar data, Journal of Atmospheric and Oceanic Technology, 27, 1265–1285, https://doi.org/10.1175/2010JTECHA1407.1, 2010.

Lawson, R. P., and P. Zuidema.: Aircraft microphysical and surface-based radar observations of summertime arctic clouds, J. Atmos. Sci., 66, 3505–3529, https://doi.org/10.1175/2009JAS3177.1, 2009.

Lhermitte, R.: Attenuation and Scattering of Millimeter Wavelength Radiation by Clouds and Precipitation, J. Atmos. Oceanic Technol., vol. 7, no.6, pp. 464–479, https://doi.org/10.1175/1520-0426(1990)007<0464:AASOMW>2.0.CO;2, 1990.

Mace, G. G, Sassen, K.: A constrained algorithm for retrieval of stratocumulus cloud properties using solar radiation microwave radiometer and millimeter cloud radar data, J. Geophys. Res., 105:29099–29108. https://doi.org/10.1029/2000JD900403, 2000.

Meneghini, R.: Rain-rate estimates for an attenuating radar, Radio Science, 13(3):459-470, https://doi.org/10.1029/RS013i003p00459, 1978.

Pazmany, Andrew. L., Wolde, Mengistu.: A compact airborne G-band (183 GHz) water Vapor Radiometer and retrievals of liquid cloud parameters from coincident radiometer and millimeter wave radar measurements, Microwave Radiometry & Remote Sensing of the Environment Microrad, 1- 4, 2008.

Pazmany, A. L., Mead, J. B.: Millimeter-wave solid-state cloud and precipitation radars and signal processing, 2018 IEEE Radar Conference (RadarConf18), IEEE, 2018.

Pazmany, A .L., Haimov, S. J.: Coherent Power Measurements with a Compact Airborne Ka-Band Precipitation Radar, Journal of Atmospheric & Oceanic Technology, 35(1), 2017.

Zhang, P., Chen, Y.: Attenuation Correction for Ka-band Cloud Radar Using X-band Weather Radar Data, https://doi.org/10.20944/preprints201611.0010.v1, 2016.

Seto, S., Iguchi, T.: Intercomparison of Attenuation Correction Methods for the GPM Dual-Frequency Precipitation Radar, Journal of Atmospheric & Oceanic Technology, 32(5):150310071117000, https://doi.org/10.1175/JTECH-D-14-00065.1, 2015.

Ulbrich, C.W.: The Accuracy of Rainfall Rate Measurement by Tunable Millimeter Wavelength Radar, J. Climate Appl. Meteor., vol. 22, no. 10, pp. 1824–1828, 1983.

Wang, Z.H., Teng, X., Ji, L., et al.: Research on k-Z relationship of spherical particle millimeter wave, Journal of Acta Meteorologica Sinica, 69(006):1020-1028, 2011.

Wang, Z.H., Ji, L., Huang, X.Y., et al: Simulation Study on the Attenuation Correction to Reflectivity Factor Observed with an Air-Borne W-Band Cloud Radar, Plateau Meteorology, 30(2):437-444, https://doi.org/10.3724/SP.J.1146.2006.01085, 2011.

Wu, J.X., Wei, M., Zhou, J.: Relationship between the extinction coefficient and radar reflectivity factor of non-spherical ice crystals, Journal of Remote Sensing, 17(6):1377-1395, https://doi.org/10.11834/jrs.20132337, 2013.

Yao S, He J, Wang H, et al.: The Attenuation Correction for Ka-Band Cloud Radar, 2019 International Conference on Meteorology Observations (ICMO), 2019.

https://doi.org/10.5194/amt-2021-221
Preprint. Discussion started: 17 August 2021


Atmospheric Measurement Techniques Discussions

435 Zhang, P.C.; Wang, Z.H. Study on Algorithm for Correcting Weather Radar Echo Attraction (Ⅰ): Theoretical Analysis, Plateau Meteorology,V20(1):1-5, 2001.

Zong, R., Liu, L. P., Yin, Y.: Relationship between cloud characteristics and radar reflectivity based on aircraft and cloud radar co-observations, Advances in Atmospheric Sciences (05), 1275-1286, https://doi.org/10.1007/s00376-013-2090-7, 2013.

440